Kannadasan Subramani
Senthil Kumar Alagarsamy
Pandivelan Chinnaiyan
Sathiya Narayanan Chinnaiyan

https://doi.org/10.21278/TOF.42206
ISSN 1333-1124
eISSN 1849-1391

STUDIES ON TESTING AND MODELLING OF FORMABILITY IN ALUMINIUM ALLOY SHEET FORMING

Summary

In this paper, the influence of tensile and formability parameters on the forming limit diagram is reported and a model is created to predict the forming limit strains of various grades of aluminium sheet metals. Aluminium alloys of grades AA5052, AA6061 and AA8011 with a thickness 0.8 mm, 1.0 mm and 1.2 mm have been selected for the study. Experiments are conducted to construct the forming limit diagram (FLD) for the above mentioned sheet metals. Tensile tests were conducted to evaluate strain hardening index, strength coefficient, ductility, yield strength, ultimate tensile strength, normal anisotropy, planar anisotropy and strain rate sensitivity. The fractured surfaces of the specimens were viewed with a scanning electron microscope. Using Design of Experiments (DOE), regression modelling was done by taking the tensile properties and formability parameters as input variables and the forming limit strain as response. Regression equations were created to predict the limiting strain values at the tension-tension, plane strain and tension-compression strain states. The experimentally evaluated strain values were compared with the predicted strain values and the comparison shows good agreement of the values. The Taguchi method of optimization was used to find the optimum values for the input variables and using these optimum values, the optimum forming limit strains were found. It is found that the so created regression model predicts the FLD of various grades of sheet metals by which the tedious job of experimental determination of the FLD can be avoided.

Key words: FLD, fractography, DOE, Taguchi, regression, optimization

1. Introduction

Aluminium alloys are indispensable as an important material in sheet metal industry because of their superior properties such as acceptable cost, low density, good mechanical properties, structural integrity and simple fabrication process. Aluminium alloys are used in the production of railcars, marine hulls, military vehicles and aircraft. Sheet metal fabrication industries require materials that do not undergo necking, wrinkling and fracture during the forming process so that dimensional accuracy is maintained. Tensile test is used to determine the mechanical properties of sheet metals. Important properties such as yield strength (Y), ultimate tensile strength (UTS), ductility (D), strain hardening index (n), strength coefficient

(K), normal anisotropy (r) and strain rate sensitivity (m) can be determined by using the tensile test. The forming limit diagram was introduced by Keelar [10], an extensive work was done by Goodwin [11] and the evaluation of the FLD was made simple by Hecker [12]. Strano and Colosimo [13] emphasised an approach to determine the forming limit curve based on experimental results. Their work focused on the separation of safe strains and failure strains.

In spite of such efforts to improve the experimental accuracy of determining the forming limits, it is essential to conduct a complete experimental investigation. Tigran Abovan et al. [4] created a finite element based criterion for predicting the FLD under isothermal conditions for the AA5000 series. Their findings indicate that the developed criterion predicted the forming limit for each strain path. Elangovan et al. [9] developed a model to predict the forming limit strain of perforated AA8011 alloy sheets of varying geometrical feature by using the artificial neural network. Ravikumar [14] made an attempt to correlate the crystallographic texture with the formability parameters. Korhonen [15] conducted experiments to determine the FLD along the rolling and transverse direction. They found that the measured limit strain in the case of the uniaxial tension is well predicted by the Rice-Tracey theory. Kleemola [16] concluded that the inferior press behaviour of aluminium is a result of smaller r and m values. Mahdavian [17] observed that the flat punch geometry produces cups with a better surface finish. Forming limit diagrams are used to find the major limiting strain and the minor limiting strain along the tension-tension, plane strain and tension-compression regions [5]. It helps to identify the limit up to which sheet metals can be formed.

Many investigations have been reported on the sheet metal formability. However, a combined study of the construction of a FLD, the prediction of a FLD using a model and the optimization of influencing variables has not yet been carried out. The present investigation has been undertaken with the aim of establishing the forming limit diagram of three grades of aluminium sheet metals, namely AA5052, AA6061 and AA8011. This paper has attempted to create a model using the Taguchi method of DOE to predict the FLD of these grades of aluminium sheet metals and the model is compared with the experimentally evaluated forming limit strains. Also, the Taguchi method of optimization is used to identify optimum values for the formability parameters by which the optimum level of the strain rate can be predicted.

2. Experimental procedure

2.1 Material

The sheet metals chosen for this study are aluminium alloys AA5052, AA6061 and AA8011 with three different thicknesses of 1.2 mm, 1.0 mm and 0.8 mm.

Table 1 Composition of alloying elements in % of AA5052, AA6061 and AA8011

Alloying Elements	Al	Si	Fe	Mn	Mg	Cr	Sn	Ti	Pb	Ca
AA5052	96.67	0.041	0.288	0.0278	2.77	0.182	0.0049	0.0054	0.0075	0.0146
AA6061	97.73	0.247	0.42	0.033	1.16	0.138	-	0.0136	-	0.0118
AA8011	98.62	0.428	0.772	0.754	0.026	0.014	-	0.0281	-	0.0096

Commercially available sheets of AA5052, AA6061 and AA8011 of 2 mm were procured and their chemical composition is shown in Table 1. These sheets were subjected to cold rolling to get 1.2 mm, 1 mm and 0.8 mm thick sheets. Cold rolling was carried out at room temperature as it improves surface finish and shows high tolerance to the flatness of the sheet metals.

2.2 Chemical composition and microstructure

Specimens were cut out from all the sheets and were subjected to a metallographic examination. The microstructure of the three sheets is shown in Figure 1.

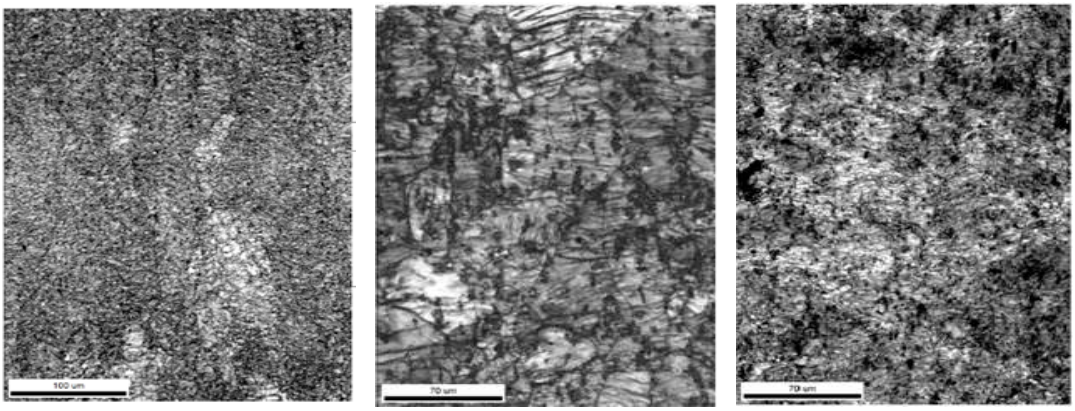

Fig. 1 Microstructure of 0.8 mm thick AA5052, AA6061, AA8011

In AA5052, the main alloying element is magnesium and in AA6061, the main alloying elements are magnesium and silicon. The concentration of magnesium in AA5052, AA6061 and AA8011 is 2.77, 1.16 and 0.026 per cent, respectively. The strength of aluminium alloy is increased by adding magnesium to aluminium without affecting ductility. This also results in better corrosion resistance and weldability. In the case of AA8011 and AA6061, the concentration of manganese is high, which increases strength, since strength decreases at lower magnesium levels. The most common impurity present in aluminium is iron. During the production of aluminium alloys, Fe readily dissolves in all molten stages as it has high solubility in molten aluminium. The silicon concentration is high in AA8011 when compared to AA5052 and AA6061. Silicon improves corrosion resistance and fluidity of the molten alloy. In AA8011, the main alloying element is lithium. It has lower density and can be added to aluminium in sufficient quantities resulting in low density and it also exhibits higher stiffness.

The microstructure of AA5052, AA6061 and AA8011 with a thickness of 0.8 mm, 1 mm and 1.2 mm shows cold work and grains in the elongated state. Recrystallization has not taken place throughout the microstructure. The microstructure of AA5052 shows smaller amounts of intermetallics. The AA6061 microstructure shows a congruent phase with evenly distributed Mg_2Si. The AA8011 microstructure shows uniformly distributed intermetallic $CaAl_4$ and $CaSi_2$.

2.3 Tensile Test

The test specimens for the tensile test were prepared as per ASTM E8/E8M -13 Standards. They were cut by Concord wire cut EDM and one specimen is shown in Figure 2. The specimens were prepared by cutting the chosen sheet metal in three different directions, namely at 0° (parallel), 45° (diagonal) and 90° (perpendicular) to the rolling direction [3]. The tensile test was performed on these specimens in 50 KN Tinius Olsen Universal Testing Machine with a strain rate of 1 mm/min.

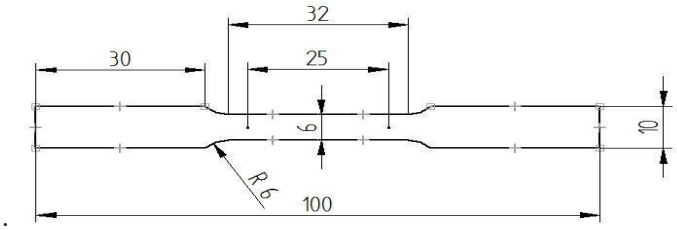

Fig. 2 ASTM E8/E8M – 13 tensile test specimen

Load versus extension data are obtained. Formability is a system characteristic which depends on material quality, chemical composition, thickness, strain hardening exponent, strength coefficient, ductility, normal anisotropy, planar anisotropy, and strain rate sensitivity. Using the tensile test, yield strength, ultimate tensile strength, ductility, true stress and true strain are determined along 0°, 45° and 90° to the rolling direction. Using the stress-strain curve of the tensile tests, the strength coefficient and the strain hardening exponent are determined along 0°, 45° and 90° to the rolling direction. The results of the tensile test are given in Table 2.

Table 2 Tensile properties of various grades of aluminium sheet metals

Sheet metal thickness	Orientation relative to rolling direction	UTS (Mpa)	Young's modulus (Mpa)	Yield strength (Mpa)	Elongation at break at non-proportional elongation	Strain hardening exponent (n-value)	Strength co-efficient K	Strain Rate sensitivity m
AA5052 0.8 mm	0◦	203	26634.47	181.06	0.0553	0.10168	195.63907	0.487
	45◦	195	27002.93	173.71	0.05998	0.15049	253.306	0.3910
	90◦	185	25201.89	163.24	0.0683	0.139	290.618	0.2718
	Average*	195	26460.56	172.93	0.0609	0.135415	248.2174	0.3852
AA5052 1 mm	0◦	144	19313.33	125.24	0.07984	0.3174	406.5362	0.64
	45◦	162	22293.75	143.01	0.07284	0.01349	406.5362	0.5929
	90◦	336	27666.87	302.13	0.06431	0.01349	306.0586	0.4278
	Average*	201	22891.91	178.34	0.0724	0.08948	396.41486	0.5289
AA5052 1.2 mm	0◦	145	27496.80	121.10	0.0576	0.07351	194.09041	0.305
	45◦	135	21369.96	119.81	0.0505	0.17315	264.6574	0.29
	90◦	136	22892.79	117.09	0.0608	0.07726	183.347	0.21
	Average*	138	23282.38	119.45	0.0548	0.1242675	226.68806	0.0.2738
AA6061 0.8 mm	0◦	535	38998.91	438.37	0.049326	0.09256	750.001	0.358
	45◦	557	33192.547	442.45	0.052824	0.15433	961.29455	0.2941
	90◦	555	37247.037	399.08	0.0599	0.04767	670.43712	0.22
	Average*	551	35657.763	430.53	0.0537	0.11222	835.7613	0.2915
AA6061 1 mm	0◦	476	33167.863	350.24	0.05606	0.1221	736.2963	0.656
	45◦	452	28426.154	185.79	0.05042	0.10273	654.014	0.273
	90◦	482	31346.105	281.11	0.0582772	0.16709	854.286	0.261
	Average*	466	30341.569	250.73	0.05379	0.12363	724.65288	0.366
AA6061 1.2 mm	0◦	444	29451.897	282.42	0.06337	0.17065	789.8222	0.45
	45◦	439	27580.07	296.89	0.0721	0.1692	776.4801	0.33
	90◦	246	42594.854	168.84	0.0822	0.0796	335.08006	0.254
	Average*	392	31801.726	261.26	0.0725	0.14718	669.4656	0.341
AA8011 0.8 mm	0◦	238	30582.645	202.2	0.04980	363.42977	0.10497	0.497
	45◦	249	36589.176	232.55	0.04707	328.34062	0.06609	0.356
	90◦	256	34328.277	235.52	0.055845	372.1522	0.08972	0.294
	Average*	248	34522.319	225.71	0.04995	348.0658	0.0817175	0.376
AA8011 1 mm	0◦	194	28494.113	177.37	0.0551733	291.23085	0.09749	0.671
	45◦	208	32668.526	184.38	0.05236	336.70546	0.11468	0.44
	90◦	200	31277.102	186.51	0.049939	284.25412	0.0818	0.36
	Average*	203	31277.067	183.16	0.05246	312.223973	0.1021625	0.4777
AA8011 1.2 mm	0◦	191	27093.508	168.73	0.050247	271.48172	0.08508	0.6471
	45◦	185	26109.471	173.62	0.043296	265.79323	0.08444	0.482
	90◦	191	43193.453	157.83	0.0657744	258.41906	0.07219	0.35
	Average*	188	30626.47	168.45	0.0506534	265.371	0.08153	0.4903

The width and the thickness of the tensile samples were measured by using a digital Vernier caliper with an accuracy of 0.02 mm. The plastic strain ratio is calculated by using expression 1,

$$r = \frac{\ln\left(\frac{w_i}{w_f}\right)}{\ln\left(\frac{t_i}{t_f}\right)} \tag{1}$$

where,

- w_i and t_i are the width and the thickness of the specimen before conducting the tensile test,
- w_f and t_f are the width and the thickness of the specimen after completing the tensile test.

Average values of the strain hardening exponent (n_{av}), the strength coefficient (K_{av}), and normal anisotropy (r_{av}) are calculated from the *n, K* and *r* values obtained along 0°, 45° and 90° to the rolling direction using the expressions given below as in [2].

$$n_{av} = (n_0 + 2n_{45} + n_{90}) / 4 \quad (2)$$

$$K_{av} = (k_0 + 2k_{45} + k_{90}) / 4 \quad (3)$$

$$r_{av} = (r_0 + 2r_{45} + r_{90}) / 4 \quad (4)$$

Planar anisotropy (Δr) is calculated using the following expression

$$\Delta r = (r_0 + r_{90} - 2r_{45}) / 2 \quad (5)$$

Strain rate sensitivity is calculated by conducting a tensile test using the specimens prepared as per ASME E51 standards from the sheet metals using a wire cut EDM along 0°, 45° and 90° to the rolling direction.

The formability parameters obtained from the tensile test for AA5052, AA6061 and AA8011 with a thickness of 0.8mm, 1mm and 1.2mm are given in Table 3.

Table 3 Formability parameters for various grades of aluminium sheet metals

Sheet metals	Thickness (mm)	*R*			Normal anisotropy r_{av}	Planar anisotropy Δr
		0˚	45˚	90˚		
AA5052	0.8	0.1933	0.1110	0.1833	0.14965	0.0773
AA5052	1	0.1078	0.1065	0.1555	0.11907	0.02525
AA5052	1.2	0.1403	0.1825	0.2077	0.17975	-0.0055
AA6061	0.8	0.1376	0.151`	0.294	0.1834	0.0648
AA6061	1	0.3572	0.1235	0.161	0.1913	0.1356
AA6061	1.2	0.1635	0.2132	0.5252	0.2787	0.1311
AA8011	0.8	0.1117	0.4179	0.1355	0.2707	-0.2943
AA8011	1	0.2629	0.3905	0.450	0.3734	-0.0340
AA8011	1.2	0.1052	0.1004	0.2588	0.1412	0.0816

2.4 Forming limit diagram (FLD)

A typical die and punch set up was designed as shown in Figure 3 and was used in a hydraulic press with double action having a capacity of 30 ton to determine the formability of aluminium sheets.

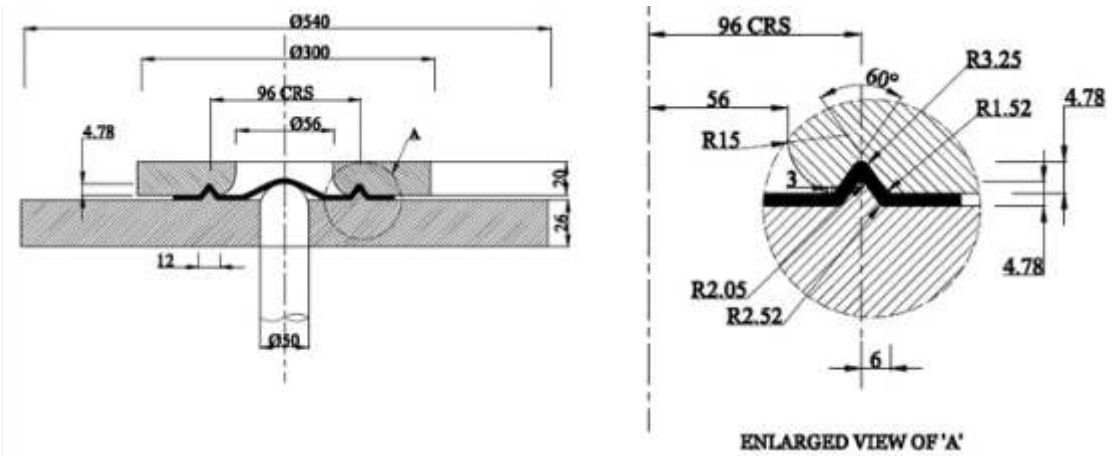

Fig. 3 A typical die punch setup

Specimens were sheared from the aluminium sheet metals AA5052, AA6061 and AA8011 with a thickness of 0.8 mm, 1.0 mm, and 1.2 mm. Specimen sizes were 110×110 mm, 110×100 mm, 110×90 mm, 110×80 mm, 110×70 mm, 110×60 mm, 110×50 mm, 110×40 mm, 110×30 mm and 110×20 mm. All the samples were laser marked with circles 2 mm in diameter in a rectangular array and were formed up to the point of fracture using the hydraulic press. Sheet specimens were subjected to different states of strain namely tension-tension, plane strain and tension-compression because of the varying width. During formation, the circles were distorted to ellipses. A travelling microscope (Vernier type) with an accuracy of 0.01 mm was used to measure dimensions of the ellipses. The true major strain and the true minor strain were calculated using the formulae as in [2],

$$\text{True major strain} = \ln(\text{Final } D \text{ major/ original diameter}) \tag{6}$$

$$\text{True minor strain} = \ln(\text{Final } D \text{ minor/ original diameter}) \tag{7}$$

The true major strain and the true minor strain were measured in the necked region, the fractured region and the safe region. The forming limit diagram was drawn using the true minor strain on abscissa and the true major strain on the ordinate. The safe region was identified by drawing a curve using the strain values obtained in the necked region. The strain states above the curve represent failure. The strain states below the curve represent the safe region. The FLD for the 1.2 mm thick AA5052 is shown in Figure 4.

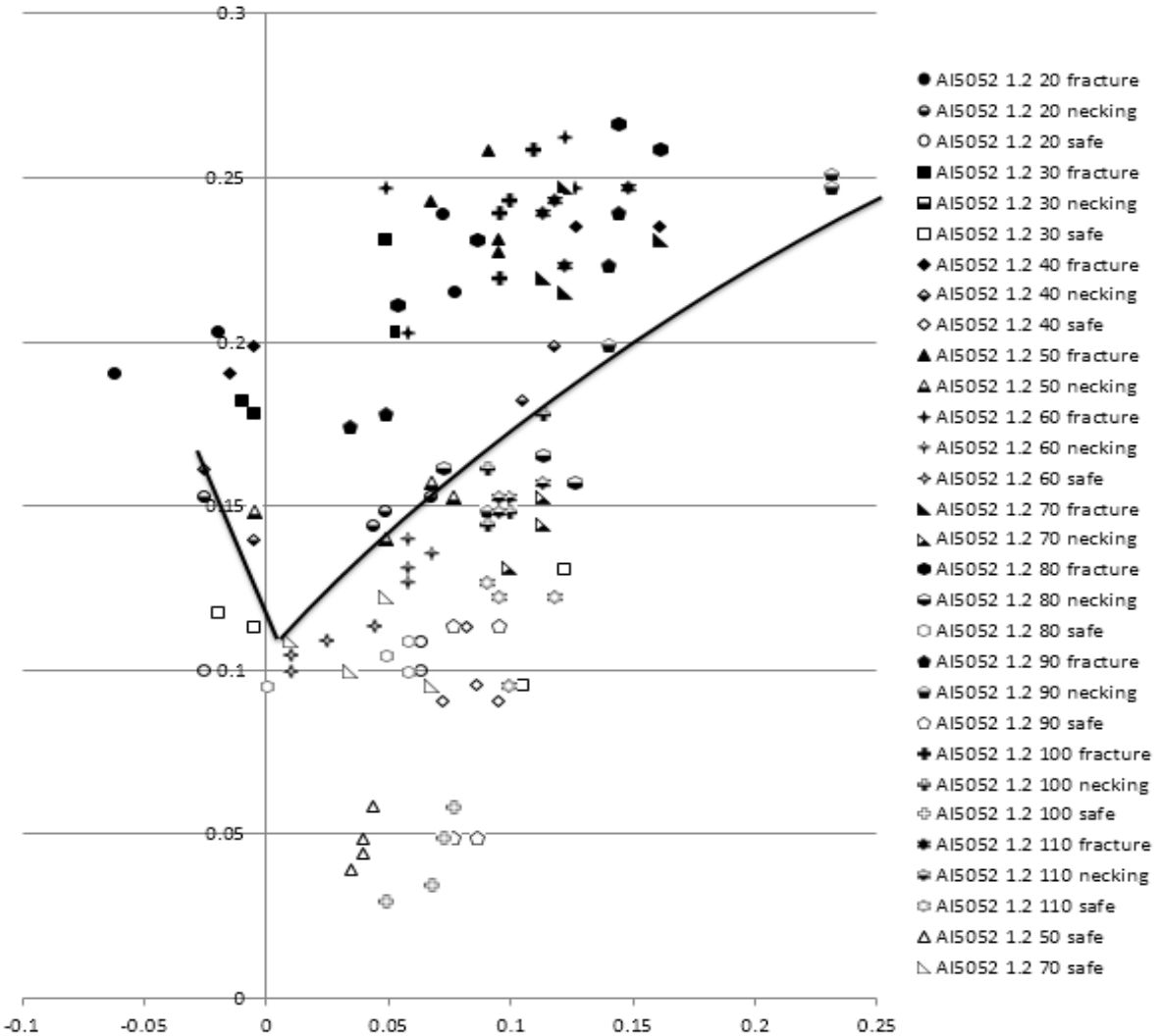

Fig. 4 Forming limit diagram of 1.2 mm thick AA5052

2.5 Fractography

A Scanning Electron Microscope (SEM) was used to explore the type of fracture in the various grades of sheet metals as shown in Figure 5. Specimens were prepared by cutting the region very close to the origin of fracture. The fracture characteristics were studied to identify the nature of fracture. In addition, the relationship between characteristics and formability was analyzed.

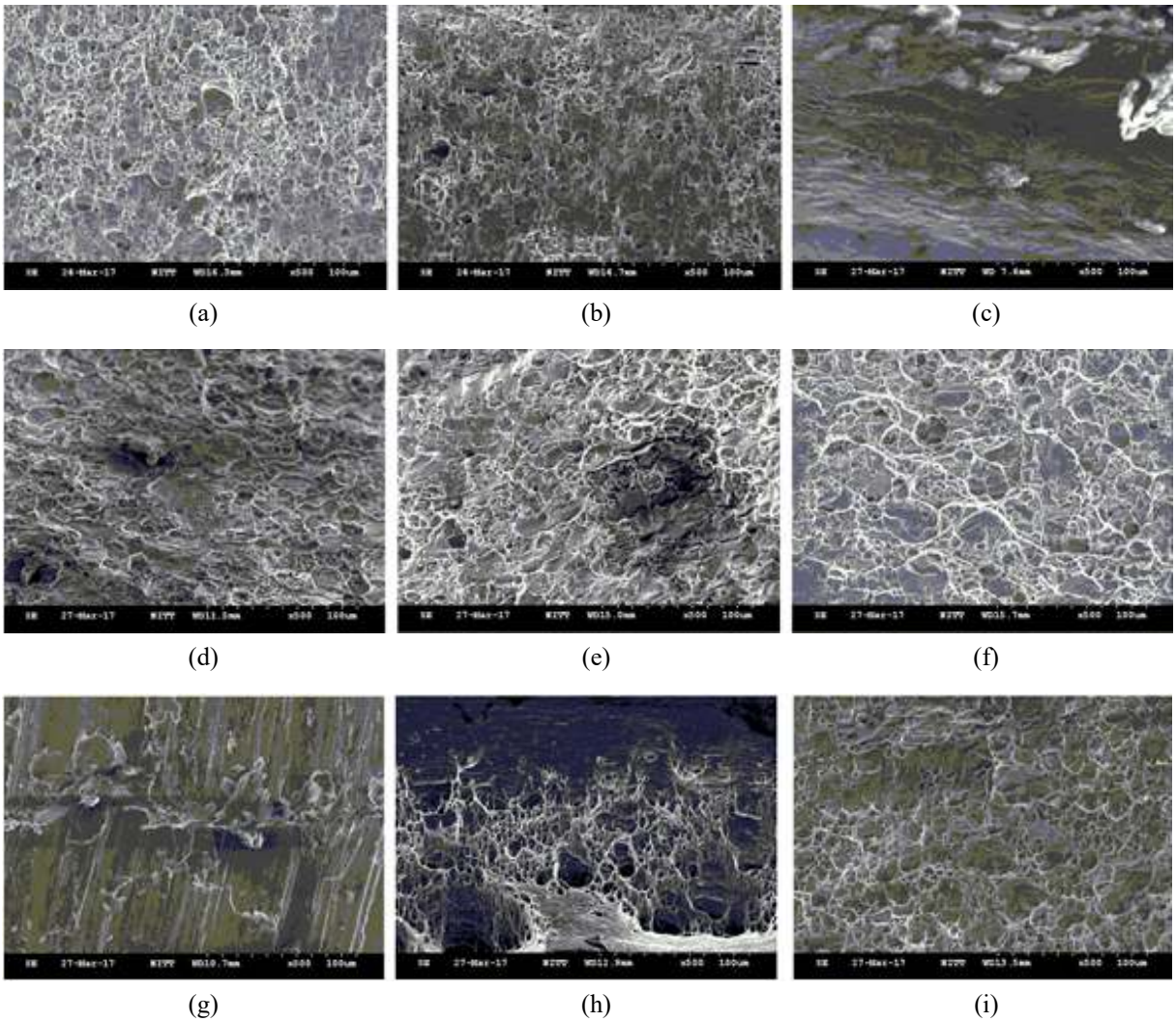

(a) (b) (c)

(d) (e) (f)

(g) (h) (i)

Fig. 5 SEM images of (a) AA5052 0.8 mm (b) AA5052 1.0 mm (c) AA5052 1.2 mm (d) AA6061 0.8 mm (e) AA6061 1.0 mm (f) AA 6061 1.2 mm (g) AA8011 0.8 mm (h) AA8011 1.0 mm (i) AA8011 1.2 mm

2.6 Modelling the formability

Modelling is essential for any experimental and theoretical calculation aiming to improve the quality of results. Design matrix for modelling was selected using Design of Experiment (DOE). The modelling was done using the Taguchi method which helps in reducing the number of experiments. The statistical analysis was done using the Minitab 14 software which uses the Taguchi approach. In the present formability analysis, seven operating parameters, i.e. *n, m, r, D, K, Y* and *UTS* were each selected at three levels to evaluate the forming limit strain. Using DOE, L_{27} orthogonal arrays were constructed. The significance of interaction terms was evaluated using L_{27}OA. The experimental forming limit strain was used as a response variable. The Taguchi analysis leads to the prediction of the forming limit strain. The percentage error between the experimentally evaluated forming

strain and the forming strain predicted by the model is shown in Table 4. A general regression for the model was performed using the Minitab software. The least square method was used in this study which minimizes the sum of squared residuals to derive the equation. The regression equation created by the Taguchi analysis for the minor strain at the tension-tension strain state of the 0.8 mm thick AA6061 is given below, which predicts the strain value.

Regression equation

$$F_{TTm} = 0.0320 + 0.1231\ n + 0.0230\ m + 0.0644\ r + 0.879\ D + 0.000001\ K - 0.000054\ Y + 0.000125\ UTS \quad (8)$$

Table 4 Design modelling for the 0.8 mm thick AA6061

n	m	r	D	K	Y	UTS	F_{TT}	F_{TT} PREDICTED	% ERROR
0.09256	0.358	0.1376	0.0493	750	438.37	535	0.14	0.147777296	-5.55521
0.09256	0.358	0.1376	0.0493	961.3	442.45	557	0.143	0.150518276	-5.25754
0.09256	0.358	0.1376	0.0493	670.4	399.08	555	0.146	0.152319356	-4.32833
0.09256	0.2941	0.151	0.0528	750	438.37	535	0.149	0.150247056	-0.83695
0.09256	0.2941	0.151	0.0528	961.3	442.45	557	0.152	0.152988036	-0.65002
0.09256	0.2941	0.151	0.0528	670.4	399.08	555	0.155	0.154789116	0.136054
0.09256	0.22	0.294	0.0599	750	438.37	535	0.158	0.163992856	-3.79295
0.09256	0.22	0.294	0.0599	961.3	442.45	557	0.161	0.166733836	-3.56139
0.09256	0.22	0.294	0.0599	670.4	399.08	555	0.164	0.168534916	-2.76519
0.15433	0.358	0.151	0.0599	750	442.45	555	0.167	0.167841223	-0.50373
0.15433	0.358	0.151	0.0599	961.3	399.08	535	0.17	0.167894503	1.238528
0.15433	0.358	0.151	0.0599	670.4	438.37	557	0.174	0.168231943	3.314975
0.15433	0.2941	0.294	0.0493	750	442.45	555	0.171	0.166263323	2.769987
0.15433	0.2941	0.294	0.0493	961.3	399.08	535	0.168	0.166316603	1.002022
0.15433	0.2941	0.294	0.0493	670.4	438.37	557	0.165	0.166654043	-1.00245
0.15433	0.22	0.1376	0.0528	750	442.45	555	0.162	0.157563363	2.738665
0.15433	0.22	0.1376	0.0528	961.3	399.08	535	0.159	0.157616643	0.870036
0.15433	0.22	0.1376	0.0528	670.4	438.37	557	0.156	0.157954083	-1.25262
0.04767	0.358	0.294	0.0528	750	399.08	557	0.16	0.160271657	-0.16979
0.04767	0.358	0.294	0.0528	961.3	438.37	555	0.163	0.158111297	2.999204
0.04767	0.358	0.294	0.0528	670.4	442.45	535	0.16	0.155100077	3.062452
0.04767	0.2941	0.1376	0.0599	750	399.08	557	0.157	0.154970697	1.29255
0.04767	0.2941	0.1376	0.0599	961.3	438.37	555	0.154	0.152810337	0.772508
0.04767	0.2941	0.1376	0.0599	670.4	442.45	535	0.151	0.149799117	0.795287
0.04767	0.22	0.151	0.0493	750	399.08	557	0.148	0.144811957	2.154083
0.04767	0.22	0.151	0.0493	961.3	438.37	555	0.145	0.142651597	1.619588
0.04767	0.22	0.151	0.0493	670.4	442.45	535	0.142	0.139640377	1.661706

2.7 Optimization of formability

The optimization was done using the Taguchi method. In this method, the main effect plots indicate the influencing parameters on the forming limit strains. The mean of means obtained by the Taguchi analysis is a plot of the response and the input variables. From the plots, the optimum level is identified. By using this optimum level for each parameter, the optimized value for the forming limit strain is given by the mean value.

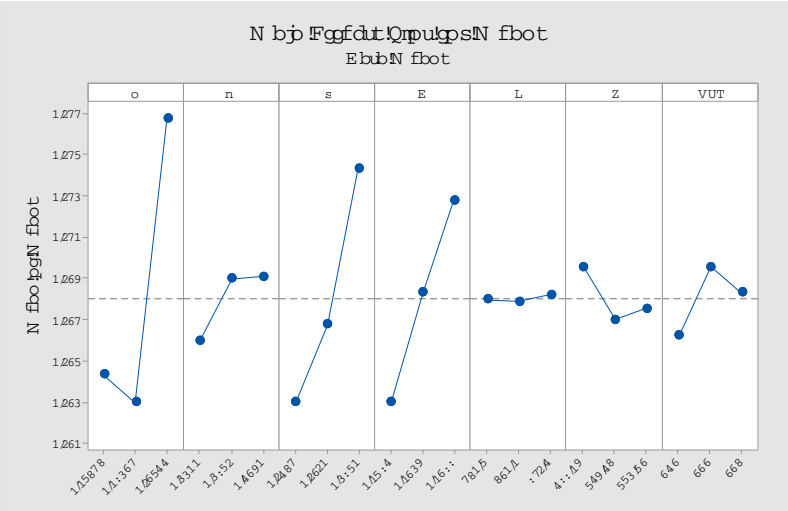

Fig. 6 The Taguchi analysis - the mean of means

Table 5 Response table for means and factor levels for predictions

Level	*n*	*M*	*r*	*D*	*K*	*Y*	*UTS*
1	0.1533	0.155	0.152	0.152	0.157	0.1586	0.1552
2	0.152	0.158	0.1558	0.1573	0.1569	0.156	0.1586
3	0.1658	0.1581	0.1633	0.1618	0.1572	0.1566	0.1573
Delta	0.0138	0.0031	0.0113	0.0098	0.0003	0.0026	0.0033
Rank	1	5	2	3	7	6	4
Factor levels for predictions	0.15433	0.358	0.294	0.0599	961.3	399.08	555

Mean = 0.1774. This mean is the optimized strain predicted by Taguchi analysis.

The minor strain in the tension-tension strain state for the 0.8 mm thick AA6061 is 0.1740 and was determined experimentally. For the same sheet in the same strain state, the optimum minor strain is 0.1774.

3. Results and Discussion

3.1 Chemical composition and microstructure

In AA6061, the concentrations of Mg, Mn, Si and Fe are moderate when compared to other grades of aluminium sheet metals. The presence of medium sized grains to slightly larger grains of Mg_2Si as well as excellent grain orientation and congruent phase lead to good formability. In AA5052, the concentration of magnesium is high and the concentrations of Mn, Si and Fe are low when compared to other grades of aluminium sheet metals. The presence of a larger grain size, favourable grain orientation and fewer amounts of intermetallics lead to good formability. In AA8011, the concentration of Mg is low and the concentrations of Mn, Si and Fe are high when compared to other grades of aluminium sheet metals. The presence of smaller grains, favourable grain orientation and the presence of intermetallics $CaAl_4$ and $CaSi_2$ lead to moderate formability.

3.2 Tensile properties and limiting strain

In the 0.8 mm thick AA5052, the limiting major strain is 21.5%, for a limiting minor strain of 15%. The limiting major strain is 1.57 times the *n* value. The 1 mm thick AA5052 has a limiting major strain of 16%, which is 1.78 times the *n* value. The 1.2 mm thick AA5052 has a limiting major strain of 21.3%, which is 1.72 times the *n* value. In the 0.8 mm thick AA6061, the limiting major strain is 18.1%, for a limiting minor strain of 15%. The

limiting major strain is 1.62 times the *n* value. The 1 mm thick AA6061 has a limiting major strain of 21.1%, which is 1.72 times the *n* value. The 1.2 mm thick AA6061 has a limiting major strain of 23.5%, which is 1.6 times the *n* value. In the 0.8 mm thick AA8011, the limiting major strain is 14.6% for a limiting minor strain of 15%. The limiting major strain is 1.8 times the *n* value. The 1 mm thick AA8011 has a limiting major strain of 18.2%, which is 1.77 times the *n* value. In the 1.2 mm thick AA8011, the limiting major strain is 16.13%, which is 2 times the *n* value.

The 1 mm thick AA5052 has a lower *n* value which results in lower formability. The 0.8 mm and 1.2 mm thick AA5052 specimens have a higher *n* value which results in better formability. In AA6061, as the sheet thickness increases, the *n* value increases. The increase in the *n* value results in better formability. The 0.8 mm and 1.2 mm thick AA8011 specimens have a lower *n* value which results in lower formability. The 1 mm thick AA8011 has a higher *n* value which results in better formability. In general, it can be said that for all the aluminium sheet metals that as the *n* value increases the limiting strain also increases in the tension-tension strain state as reported in [14]. The strain hardening index is a parameter which shows the ability of sheet metals to be stretched and drawn as described in [7]. Higher *n* value infers higher drawability. The 1.2 mm thick AA6061 sheet metal has the highest average *n* value among all the nine sheet metal specimens, which results in the highest limiting strain in the tension-tension strain state. For this sheet, the *UTS* and the *K* value are higher along the rolling direction and yield strength is higher along 45^0 to the rolling direction.

3.3 Formability parameters and limiting strain

The important formability parameters such as normal anisotropy (*r*) and planar anisotropy (Δr) determined by the tensile test are presented in Table 3. The 1 mm thick AA5052 has a lower *r* value which results in lower formability. The 0.8 mm and 1.2 mm thick AA5052 have higher *r* values which results in better formability. In AA6061, as the sheet thickness increases, the *r* value increases. The increase in the *r* value results in better formability. The 0.8 mm and 1.2 mm thick AA8011 have lower *r* values which results in lower formability. The 1 mm thick AA8011 has a higher *r* value which results in better formability. The 1 mm thick AA8011 sheet metal has the highest *r* value among the nine sheet metals and it possesses the highest limiting strain in the tension-compression strain state. This implies that as the *r* value increases, the limiting strain also increases in the tension-compression strain state as reported in [1]. Sheet metal with a high *r* value has high drawability as it shows good resistance to thinning in the thickness direction during forming as presented in [3]. Planar anisotropy (Δr) is low for all the sheet metals studied and it is very low for the 1.2 mm thick AA5052 sheet metal. This shows that the earing tendency decreases during the drawing process for all the sheet metals, since the earing during deep drawing is related to planar anisotropy as presented in [1]

3.4 Fractography

The SEM images of all the sheet samples show a similar type of features like voids, dimples and cavities but with variation in size and shapes. In AA6061, the average void size is 5.49 μm. The presence of bigger size voids and a large number of voids indicate the ductile type of fracture resulting in good formability. For example, the limiting major strain at a minor strain of 15% is 23.5%. In the case of AA5052, whose formability is slightly lower than that in AA6061, the average void size is 5.38 μm and it shows a limiting major strain of 21.5% at a minor strain of 15%.. In the case of AA8011, whose formability is lower than that in AA5052 and AA6061, the average void size is 4.16 μm and it shows a limiting major strain of 18.2% at a minor strain of 15%. The average void size and the formability measured for these sheets are in good correlation.

3.5 Modelling and optimization

The percentage variations between the experimental strain and the model predicted strain and the optimized strain for different strain states are shown in Table 6. In the AA5052 sheet metal of 0.8 mm, 1 mm and 1.2 mm in thickness, the percentage error varies from 1.23 to 8.01, 0.62 to 5.46 and 0.43 to 4.7, respectively, in different strain states. In the AA6061 sheet metals of 0.8 mm, 1 mm and 1.2 mm in thickness, the percentage error varies from 2.21 to 4.5, 0.52 to 5.35 and 1.29 to 4.91, respectively, in different strain states. In the AA8011 sheet metals of 0.8 mm, 1 mm and 1.2 mm in thickness, the percentage error varies from 0.74 to 9.23, 2.58 to 6.77 and 0.85 to 5.8, respectively, in different strain states.

Table 6 Comparison of limiting strain for various grades of aluminium sheet metals in different strain states

Sheet metal thickness	Strain state	Strain type	Experimental strain	Model predicted strain	Percentage error	Optimized strain
AA5052 0.8 mm	Tension - tension	Minor strain	0.223	0.2121	4.85	0.2311
		Major strain	0.227	0.2161	4.65	0.2351
	Plane strain	Major strain	0.135	0.124	8.01	0.1431
	Tension - compression	Minor strain	0.067	0.066	1.23	0.06771
		Major strain	0.148	0.137	7.31	0.1561
AA5052 1 mm	Tension - tension	Minor strain	0.161	0.16	0.62	0.16119
		Major strain	0.166	0.163	1.64	0.163
	Plane strain	Major strain	0.09	0.087	2.97	0.0887
	Tension - compression	Minor strain	0.05	0.047	5.46	0.047
		Major strain	0.131	0.1282	2.07	0.1281
AA5052 1.2 mm	Tension - tension	Minor strain	0.231	0.228	1.22	0.2359
		Major strain	0.243	0.2419	0.43	0.2408
	Plane strain	Major strain	0.124	0.1223	1.32	0.1254
	Tension - compression	Minor strain	0.025	0.0238	4.7	0.0226
		Major strain	0.161	0.1599	0.65	0.1588
AA6061 0.8 mm	Tension - tension	Minor strain	0.174	0.16823	3.31	0.1774
		Major strain	0.186	0.1818	2.21	0.1937
	Plane strain	Major strain	0.112	0.107	4.55	0.1192
	Tension - compression	Minor strain	0.025	0.0243	2.52	0.02578
		Major strain	0.135	0.1308	3.05	0.1427
AA6061.1 mm	Tension - tension	Minor strain	0.135	0.128	5.05	0.1357
		Major strain	0.2077	0.2064	0.59	0.2077
	Plane strain	Major strain	0.123	0.1223	0.52	0.1238
	Tension - compression	Minor strain	0.025	0.0239	4.26	0.02547
		Major strain	0.135	0.1277	5.35	0.1432
AA6061 1.2 mm	Tension - tension	Minor strain	0.169	0.1655	2.02	0.1698
		Major strain	0.27	0.2616	3.07	0.2756
	Plane strain	Major strain	0.147	0.145	1.29	0.1483
	Tension - compression	Minor strain	0.046	0.0437	4.91	0.0475
		Major strain	0.169	0.1655	2.02	0.1695
AA8011 0.8 mm	Tension - tension	Minor strain	0.161	0.1535	4.64	0.1691
		Major strain	0.166	0.158	7.5	0.1741
	Plane strain	Major strain	0.081	0.0735	9.23	0.0891
	Tension - compression	Minor strain	0.04	0.039	2.39	0.04
		Major strain	0.113	0.1121	0.74	0.1138
AA8011 1 mm	Tension - tension	Minor strain	0.194	0.188	3.19	0.2007
		Major strain	0.199	0.1924	3.31	0.2053
	Plane strain	Major strain	0.103	0.096	6.77	0.1092
	Tension - compression	Minor strain	0.035	0.0336	4.75	0.0357
		Major strain	0.178	0.171	3.77	0.1847
AA8011 1.2 mm	Tension - tension	Minor strain	0.161	0.151	5.8	0.1685
		Major strain	0.166	0.1594	3.95	0.17088
	Plane strain	Major strain	0.081	0.0803	0.84	0.0815
	Tension - compression	Minor strain	0.051	0.0504	1.05	0.05158
		Major strain	0.1	0.0988	1.64	0.10058

Twenty % of all sheets included in the study have a percentage error less than 1, 30% of sheets have a percentage error between 1 and 3, 37% of sheets have a percentage error between 3 and 5, and 13% of sheets have a percentage error between 5 and 10. This shows that a total of 87% of sheets have an error less than 5%, which indicates that the experimental values and the model predicted values are in good agreement. The strain values obtained from the optimization are slightly higher than the experimental and the model predicted values. This shows that the forming limit increases in all sheet metals when the Taguchi method of optimization is incorporated into various grades of sheet metals.

The correlation between the experimentally evaluated forming limit strains and the model predicted forming limit strains for the various grades of sheet metals with different thicknesses are shown in Figure 7. It is found that the experimental FLD and the model predicted FLD are almost in line with each other.

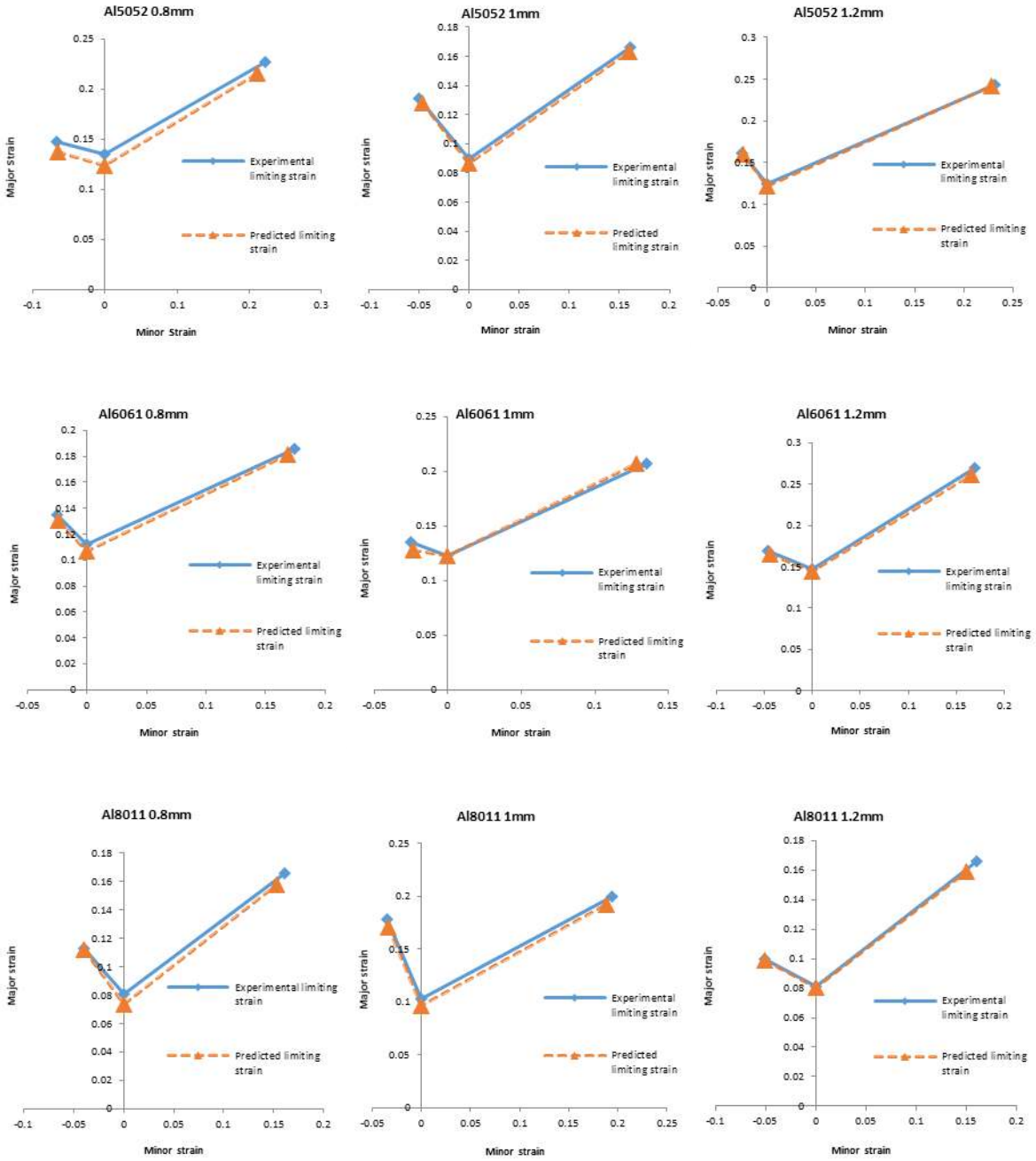

Fig. 7 Variation of FLD of various grades of aluminium sheet metals between the experimental and model predicted limiting strains

4. Conclusions

The chemical composition of the studied sheet metals reveals that high Mg concentration and low Mn, Si and Fe concentrations result in better formability and the microstructure shows that the presence of larger grain size results in good formability. The tensile test results show that the ductility range lies between 5% and 7.25% for the various grades of aluminium sheet metals, which suggests that high stretchability is possible. The average n values and *k* values of these sheet metals are higher, which results in better formability. The planar anisotropy *(*Δr) values of all the sheets are low, which indicates that earing is low. The SEM images show shallow dimples and deep voids with ductile types of fractures. The results also show that the 1.2 mm thick AA6061 has the highest major limiting strain at a particular minor strain for the tension-tension, plane strain and tension-compression strain states; therefore, the workability range of this sheet metal is good. The regression model equations in different strain conditions are constructed and the forming limit strain is predicted, which is in good agreement with the experimentally evaluated forming limit strain. The Taguchi analysis carried out in this study shows the optimum forming limit strain, and it is observed that the strain hardening index and normal anisotropy are the most influencing factors in determining the forming limit strains. It is also concluded that the optimization of formability results in a better forming limit of various grades of sheet metals. Finally, the forming limit of a particular sheet metal can be predicted by applying the tensile test factors on the corresponding regression model equations, by which the experimental determination of the FLD can be avoided.

REFERENCES

[1] Narayanasamy, R.; Sathiyanarayanan, C. (2007), Experimental Analysis and evaluation of Forming Limit diagram Interstitial Free steels. Materials and Design 28; 1490-1512. https://doi.org/10.1016/j.matdes.2006.03.010

[2] Chandrasekar, K.; Narayanasamy, R.; Velmanirajan, K. (2014), Experimental investigations on Micro structure and Formability of Cryorolled AA5052 sheets. Materials and Design 53; 1064-1070. https://doi.org/10.1016/j.matdes.2013.08.008

[3] Narayanasamy, R.; Sathiyanarayanan, C. (2005), Forming limit diagram for industrial free steels Part 1, Materials Science and Engineering. A 399; 292-307. https://doi.org/10.1016/j.msea.2005.04.004

[4] Tigram Abovyan, Ghassan, T. Kridli; Peter, A Friedman; Georges Ayoub (2015), Formability Prediction of aluminium sheet alloy under Isothermal Forming Conditions. Journal of Manufacturing Process 20; 406-413. https://doi.org/10.1016/j.jmapro.2014.08.003

[5] Narayanasamy, R.; Ravindran, R.; Manonmani, K.; Satheesh, J. A. (2009), Crystallographic texture perspective formability investigation of Aluminium 5052 Alloy sheets at various Annealing temperatures. Materials and Design 30; 1804-1817. https://doi.org/10.1016/j.matdes.2008.09.011

[6] Picu, R. C.; Vincze, G.; Ozturk, F. (2005), Strain rate sensitivity of the commercial aluminium alloy AA5182.0 Materials Science and Engineering A390; 334-343. https://doi.org/10.1016/j.msea.2004.08.029

[7] Narayanasamy, R.; Sathiyanarayanan, C. (2004), Report of FLD on IF Steels submitted to TISCO, National Institute of Technology, Tiruchirappalli 620015, Tamil Nadu, India.

[8] Vasin, R. A.; Enikeev, F. U.; Mazurski, M.I. (1998), Method to determine the strain rate sensitivity of a super plastic material from the initial slopes of its stress strain curves. Journal of Materials Science 33; 1099-1103. https://doi.org/10.1023/A:1004348919985

[9] Elangovan, K.; Sathiyanarayanan, C.; Narayanasamy, R. (2010), Modelling of forming limiting diagram of perforated commercially pure Aluminium sheets using Artificial Neural Network. Computational Materials Science 47(4), 1072-1078. https://doi.org/10.1016/j.commatsci.2009.12.016

[10] Keelar, S. P.; (1965) Determination of forming limits in automotive stampings. Sheet Met Ind; 42: 683–691. https://doi.org/10.4271/650535

[11] Godwin, G. M.; (1968), Application of strain analysis to sheet metal forming problems in the press shop. Metall Italiana; 60: 764–774. https://doi.org/10.4271/680093

[12] Hecker, S. S.; (1975) Simple technique for determining forming limit curves. Sheet Met. Ind; 52(11): pp 671-676.

[13] Strano, M.; Colosimo, B.M. (2006), Logistic regression analysis for experimental determination of forming limit diagrams, Int Journal Mach Tools Manuf; 46 (6); 673-682. https://doi.org/10.1016/j.ijmachtools.2005.07.005

[14] Ravikumar, D.; Swaminathan, K. (2013), Formability of two aluminium alloys. Material science and Technology, 15:11, 1241-1252.

[15] Korhonen, A.; Heikinheimo, E. (2013), Forming and fracture limits of aluminium alloy. Material Science and Technology, 27:11, 1694-1700.

[16] Kleemola, H.J.; Kumpalainen, J.O. (2013), Formability of aluminium and steel sheets. Journal of Metals Technology, 159-162.

[17] Mahdavian, S. M.; Tui Mei Yen Fion (2007), Effect of punch geometry in the deep drawing process of aluminium. Materials and Manufacturing Processes, 22; 898-902. https://doi.org/10.1080/10426910701451713

Submitted: 21.6.2017

Accepted: 18.10.2017

Lecturer. Kannadasan Subramani
Department of Mechanical Engineering, Govt. Polytechnic College, Tiruchirappalli, Tamilnadu, India

Assist. Professor. Senthil Kumar Alagarsamy
Department of Mechanical Engineering, University College of Engineering, Panruti, Tamilnadu, India

Assist. Professor. Pandivelan Chinnaiyan
Department of Mechanical Engineering, Vellore Institute of Technology, Vellore, Tamilnadu, India

Assist. Professor. Sathiya Narayanan Chinnaiyan
Department of Production Engineering, National Institute of Technology, Tiruchirappalli, Tamilnadu, India

APPENDIX

F_{TTm} = Forming limit minor strain at tension-tension strain state
F_{TTM} = Forming limit major strain at tension-tension strain state
F_P = Forming limit major strain at plane strain state
F_{TCm} = Forming limit minor strain at tension-compression strain state
F_{TCM} = Forming limit major strain at tension-compression strain state

AA6061 Thickness 0.8mm

F_{TTm} = 0.0359 + 0.1231 n + 0.0230 m + 0.02881 r + 0.879 D + 0.000001 K - 0.000054 Y + 0.000125 UTS ..(1)

F_{TTM} = 0.0377 + 0.1701 n + 0.0277 m + 0.03076 r + 0.865 D + 0.000000 K - 0.000070 Y + 0.000143 UTS ..(2)

F_P = -0.0243 + 0.1614 n + 0.0274 m + 0.02816 r + 0.937 D + 0.000001 K - 0.000082 Y + 0.000125 UTS ..(3)

F_{TCm} = -0.0597 + 0.1275 n + 0.0205 m + 0.01990 r + 0.443 D - 0.000001 K - 0.000034 Y + 0.000064 UTS ..(4)

F_{TCM} = -0.0133 + 0.1701 n + 0.0277 m + 0.03076 r + 0.865 D + 0.000000 K - 0.000070 Y + 0.000143 UTS ..(5)

AA6061 Thickness 1 mm

F_{TTm} =0.1736-0.0257n -0.00131m + 0.01214r -0.042D +0.000002K +0.000002Y- 0.000014UTS ..(6)

F_{TTM} = 0.2642 - 0.0232 n - 0.00766m+ 0.0225r - 0.168D + 0.000003K + 0.000008Y + 0.000013UTS ..(7)

F_P = 0.14234 - 0.01062 n - 0.00084m + 0.00463r - 0.0264D + 0.000002K + 0.000001Y + 0.000007UTS ..(8)

F_{TCm} = -0.0446 + 0.0148 n + 0.00119m - 0.00825r - 0.0180D - 0.000001K+0.000001Y + 0.000003UTS (9)

F_{TCM} = 0.1736 - 0.0257 n - 0.00131m + 0.01214r-0.042D + 0.000002K+ 0.000002 Y- 0.000014UTS (10)

AA6061 Thickness 1.2 mm

F_{TTm} = 0.1474 + 0.0363 n - 0.0088 m - 0.0174 r + 0.281 D + 0.000010 K - 0.000033 Y - 0.000023 UTS . .(11)

F_{TTM} = 0.20026 + 0.01230 n + 0.00223 m - 0.00332 r + 0.0554 D - 0.000000 K - 0.000002 Y - 0.000001 UTS ..(12)

F_P = 0.11672 + 0.01188 n + 0.00181 m - 0.00310 r + 0.0512 D + 0.000000 K - 0.000002 Y -.000001 UTS ..(13)

F_{TCm} = -0.01981 - 0.00143n + 0.00255m + 0.00605r - 0.0786D - 0.000001K- 0.000002Y + 0.000001UTS ..(14)

F_{TCM} = 0.0722 + 0.1188 n + 0.0181 m - 0.0310 r + 0.512 D + 0.000001 K - 0.000024 Y - 0.000010 UTS ..(15)

AA8011 Thickness 0.8 mm

F_{TTm} = 0.0722 - 0.389 n + 0.0164 m - 0.0051 r + 0.739 D - 0.000001 K + 0.000065 Y+ 0.000191 UTS . .(16)

F_{TTM} = 0.0772 - 0.389 n + 0.0164 m - 0.0051 r + 0.739 D - 0.000001 K + 0.000065 Y + 0.000191 UTS . .(17)

F_P = -0.0078 - 0.389 n + 0.0164 m - 0.0051 r + 0.739 D - 0.000001 K + 0.000065 Y + 0.000191 UTS ..(18)

F_{TCm} = -0.0333 + 0.476 n + 0.0342m + 0.0023r - 0.377D- 0.000013K - 0.000030K - 0.000095UTS ..(19)

F_{TCM} = 0.10412 - 0.0389 n + 0.00164 m - 0.00051 r + 0.0739 D - 0.000000 K + 0.000006 Y + 0.000019 UTS ..(20)

AA8011 Thickness 1 mm

F_{TTm} = 0.1557 + 0.5432 n + 0.00708m + 0.0534r - 1.630D + 0.000006K + 0.000075Y+ 0.000124UTS .. (21)

F_{TTM} = 0.0868 + 0.5469 n + 0.01130m + 0.0614r - 1.556D + 0.000004K+ 0.000337Y+ 0.000214UTS .. (22)

F_P = -0.0144 + 0.5470 n + 0.01158m + 0.0607r - 1.537D + 0.000004K + 0.000350Y + 0.000221UTS ..(23)

F_{TCm}= -0.0294 - 0.0527 n + 0.00099m - 0.00729r + 0.2111D + 0.000002K - 0.000032Y- 0.000016UTS . .(24)

F_{TCM} = 0.0982 + 0.5469 n + 0.01062m + 0.0657r - 1.630D - 0.000009K + 0.000269 Y+ 0.000151UTS ..(25)

AA8011 Thickness 1.2 mm

F_{TTm} = 0.086 + 0.877 n + 0.0124m + 0.0587r + 0.248D + 0.000042K - 0.000190Y - 0.000185UTS ..(26)

F_{TTM} = 0.108 + 0.848 n + 0.0065m + 0.0380r + 0.141D + 0.000009K - 0.000138Y - 0.000148UTS ..(27)

F_P = 0.07128 + 0.1074 n + 0.000994m + 0.00397r + 0.0189D + 0.000003K - 0.000013Y- 0.000011UTS ..(28)

F_{TCm} = -0.04091 - 0.1069 n - 0.000955m - 0.00396r - 0.0183D - 0.000004K + 0.000013Y+ 0.000009UTS ..(29)

F_{TCM} = 0.1129 - 0.0140 n - 0.00169m + 0.00629r + 0.0281D - 0.000025K - 0.000028Y- 0.000029UTS . .(30)

AA5052 Thickness 0.8 mm

F_{TTm} = 0.1973 + 0.1855 n + 0.0178m + 0.0135r + 0.696D - 0.000006K - 0.000186Y - 0.000180UTS ..(31)

F_{TTM} = 0.2013 + 0.1855 n + 0.0178m + 0.0135r + 0.696D - 0.000006K - 0.000186Y- 0.000180UTS ..(32)

F_P = 0.1093 + 0.1855 n + 0.0178m + 0.0135r + 0.696D - 0.000006K - 0.000186Y- 0.000180UTS ..(33)

F_{TCm} = -0.06088 - 0.05278 n + 0.00196m - 0.00125r - 0.0833D - 0.000 002K + 0.000022Y+ 0.000021UTS ..(34)

F_{TCM} = 0.1223 + 0.1855 n + 0.0178m + 0.0135r + 0.696D - 0.000006K - 0.000186Y- 0.000180UTS ..(35)

AA5052 Thickness 1 mm

F_{TTm} = 0.16263 - 0.00685 n - 0.00092m + 0.02225r - 0.0773D - 0.000004K+ + 0.000002Y + 0.00000 UTS ..(36)

F_{TTM} = 0.1589 + 0.00647 n + 0.00346m + 0.0222r- 0.0773D + 0.000007K+ 0.000002Y+ 0.000001UTS ..(37)

F_P = 0.08629 - 0.00166 n + 0.00033m + 0.0212r - 0.1312D + 0.000012K + 0.000004Y+ 0.000003UTS ..(38)

F_{TCm} = -0.0429 - 0.00647 n - 0.00346m - 0.0222r + 0.0773D - 0.000007K - 0.000002Y- 0.000001UTS . .(39)

F_{TCM} = 0.1243 + 0.00504 n + 0.00327m + 0.0231r - 0.0779D + 0.000006K + 0.000002Y + 0.000001 UTS ..(40)

AA5052 Thickness 1.2 mm

$F_{TTm} = 0.236 + 0.0448\ n + 0.0402m + 0.0513r + 0.044D + 0.000002K - 0.000214Y - 0.000077UTS$ ..(41)

$F_{TTM} = 0.2522 + 0.02303\ n - 0.00346m + 0.02392r + 0.0207D - 0.000000K - 0.000100Y - 0.000036UTS$ ..(42)

$F_{P} = 0.1297 + 0.0307\ n + 0.0178m + 0.0341r + 0.030D + 0.000001K - 0.000140Y - 0.000050UTS$ ..(43)

$F_{TCm} = -0.0367 - 0.02267\ n + 0.00334m - 0.02316r - 0.0061D - 0.000001K + 0.000103Y + 0.000047UTS$ ..(44)

$F_{TCM} = 0.1702 + 0.02303\ n - 0.00346m + 0.02392r + 0.0207D - 0.000000K - 0.000100Y - 0.000036UTS$ ..(45)